HEFAT2010
7th International Conference on Heat Transfer, Fluid Mechanics and Thermodynamics
19-21 July 2010
Antalya, Turkey

DYNAMIC THERMAL FEATURES OF INSULATED CONCRETE BRICKS

Cianfrini C., Corcione M. and Habib E.*
*Author for correspondence
Dipartimento di Fisica Tecnica
Università di Roma "La Sapienza"
Roma 00184
Italy
e-mail: emanuele.habib@uniroma1.it

ABSTRACT

Unsteady heat transfer through walls has been largely studied, being of primary importance for the prediction of building energy demand. Nevertheless, the readily available calculation methods are typically related to homogenous layers, even though hollow or insulated bricks are often used. For this reason, a study of the dynamic thermal performance of insulated concrete blocks is brought forth in the present paper. A finite-volume method is used to solve the two-dimensional equation of conduction heat transfer. An excitation consisting of a triangular temperature-pulse is used to analyse the thermal response of the bricks. The effects of both the type of concrete and the insulating filler are investigated and discussed.

INTRODUCTION

Dynamic heat transfer through building envelopes has been extensively studied, being of fundamental importance in building thermal modelling. Different methods for the calculation of the heat gain through exterior roofs and walls are described in [1]. However, as these methods apply uniquely to roofs and walls consisting of homogeneous layers, their employment is not suitable for either 2-D or 3-D transient analyses. Actually, the studies readily available in the open literature on the dynamic thermal features of non-homogeneous building components are very few.

Lacarrière et al. [2] performed an experimental study on the response of a single vertically-perforated brick subjected to a step temperature change. The results obtained showed that the layer of perforated bricks was equivalent to a homogeneous layer having a thermal effusivity slightly lower than one half of that of the solid part of the brick (terra cotta). In addition, once the effective thermal conductivity of the brick was derived from its thermal resistance, the effective heat capacity per unit volume of the brick resulted to be of the same order of that of the solid part of the brick. Sala et al. [3] measured the response factors for a three-layered wall made of (exterior to interior) an EPS insulating layer, a hollow brick layer and a gypsum layer, that was subjected to a triangular temperature-pulse. In this case the effective heat capacity per unit volume of the brick resulted to be nearly one half of that of the clay which the solid part of the brick consisted of.

As regards the numerical approach to the problem, Vijaykumar et al. [4] calculated the dynamic heat transfer effects of both solid and hollow clay tiles located upon concrete roofs in tropical climate conditions, compared with the bare concrete roof. According to the results obtained, the addition of the tiles brought to the same time lag independently of the fact that the tiles were either solid or hollow. Zhang and Wachenfeldt [5] analyzed the dynamic heat storage capacity of hollow concrete slabs. They found that, although the cavity-area fraction was nearly 50%, the heat capacity per unit volume of the equivalent homogeneous layer was about two times that of the solid part of the slab. Finally, Dos Santos and Mendes [6] studied the thermal response of a brick either solid, hollow or insulated, showing that insulated and solid bricks shared exactly the same type of time-evolution of the heat flux.

In sum, it may be seen that the problem of the dynamic behaviour of non-homogeneous building envelopes has been treated quite differently by the different authors cited above, and the results obtained are hardly comparable among each other. This has motivated the present study, whose aim is to analyse the effect of an insulating filler on the thermal behaviour of a brick. A two dimensional numerical study is performed under the assumption that the investigated brick is subjected to a triangular temperature-pulse on one side. The reference brick is chosen among those indicated in European standard EN1745 [7]. Owing to the first-approach character of the present work, the simplest brick structure available has been chosen, i.e., that denoted as B.29, which consists of a concrete masonry unit. Reference masonry material is concrete with expanded clay aggregate (CNC), whereas mineral-wool and polystyrene are the possible embedded insulating materials. The full brick, without any insulation filler, is used as reference configuration.

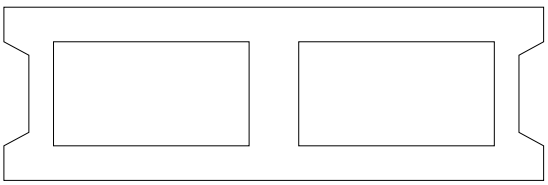

a) Concrete masonry unit EN1745 – B.29

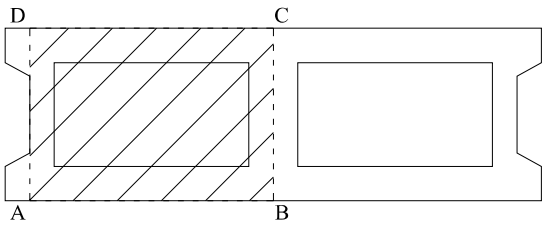

b) Computational domain

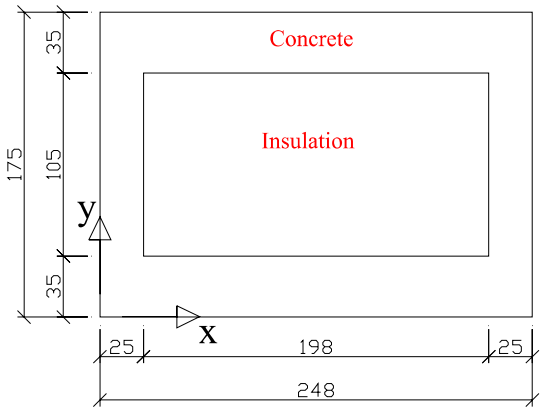

c) Dimensions of the computational domain

Figure 1 Sketch of the reference masonry unit and the computational domain (dimensions are in mm)

MATHEMATICAL FORMULATION

The reference masonry unit is sketched in Fig. 1(a). Real walls have mortar all around the block, giving fully three-dimensional thermal fields. However, as this study is meant to be a first-approach study, the effect of the mortar, the lateral edges of the brick, and the plaster layer, are neglected. The computational domain is rectangular and represents one half of the brick, as displayed in Fig. 1(b). The domain is 248 mm long, and 175 mm wide (in the main direction of the heat flux). The outer frame is made of concrete (CNC), whereas the core of the domain may consist of either concrete or an insulating filler (as said, mineral-wool and polystyrene are considered).

The temperature field is assumed to be two-dimensional. The thermal properties of the materials are considered to be constant (i.e., independent of temperature). All materials are assumed to be isotropic (indeed, construction materials have typically a low anisotropy, and, additionally, the anisotropy ellipsoid has a circular cross section with the main axis aligned to the material extrusion direction).

The thermal field equation is the Fourier's equation:

$$k\left(\frac{\partial^2 T}{\partial x^2}+\frac{\partial^2 T}{\partial y^2}\right)=c\rho\frac{\partial T}{\partial \tau} \tag{1}$$

At the junction between the different materials, heat flux conservation is imposed:

$$k_1\frac{\partial T}{\partial n}\bigg|_1=k_2\frac{\partial T}{\partial n}\bigg|_2 \tag{2}$$

Along the sides BC and AD, a zero heat flux condition is imposed for symmetry:

$$\frac{\partial T}{\partial x}=0 \tag{3}$$

On face AB the uniform triangular temperature-pulse, with a 10°C amplitude and 2h time-length displayed in Fig. 2 is used as boundary condition. On the opposite face CD, a constant uniform reference temperature T_0=20°C is imposed. The initial condition that has been assumed at time τ=0 is a uniform temperature T=20°C throughout the whole computational domain for all the simulations executed.

The triangular excitation used in the present study allows us to determine quite clearly the heat transfer response of the bricks analysed, in terms of both time-lag and decrement factor. In fact, owing to the linearity of the problem, any possible thermal excitation can be decomposed in a sequence of triangular pulses and the final solution can be given as a time convolution of the successive responses, which implies that the response to a triangular pulse is able to give a complete description of the transient behaviour of the bricks [8].

COMPUTATIONAL PROCEDURE

The governing equation (1) along with the boundary and initial conditions stated above is solved through a control-volume formulation of the finite-difference method. A first-order backward scheme is used for time stepping.

As known, the set of the discretized equations is strictly linear. Moreover, the coefficients are time-independent. Thus, the Banachiewicz-Doolittle LU factorization algorithm [9] is used to solve the temperature field without iterations.

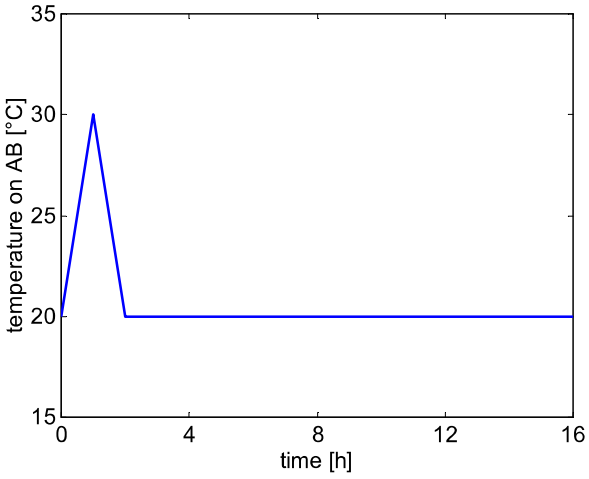

Figure 2 Temperature-pulse used as boundary condition

Mesh size	Δτ	q[W/m^2]	%	Exec. time
18x20	10"	2.7633	-0.45%	2'18"
18x40	10"	2.7567	-0.21%	5'42"
18x60	10"	2.7561	-0.19%	8'48"
28x20	10"	2.7604	-0.34%	5'17"
28x40	10"	2.7540	-0.11%	12'21"
36x40	10"	2.7530	-0.08%	19'52"
48x20	10"	2.7596	-0.31%	15'38"
48x60	10"	2.7520	-0.04%	59'09"
56x60	10"	2.7508	0.00%	1h23'20"

Table 1 Grid sensitivity analysis for CNC4 filled with polystyrene

The average heat flux through face CD is calculated as:

$$q = \frac{1}{0.248}\int_0^{0.248} k_{CNC}\frac{\partial T}{\partial y}dx \tag{4}$$

The computational code is checked against some available reference analytic solutions. Since no simple two-dimensional unsteady solution is readily available in the literature, the code is validated by comparing the numerical results with a two-dimensional steady temperature field, and a one-dimensional transient solution.

The reference steady solution is the temperature field over a rectangular domain with imposed zero temperature on three sides and a sinusoidal temperature distribution on the remaining side, given by [10]:

$$T(x,y) = T_m \frac{\sinh\left(\frac{\pi y}{L}\right)}{\sinh\left(\frac{\pi B}{L}\right)}\sin\left(\frac{\pi x}{L}\right) \tag{5}$$

where T_m is the maximum boundary temperature, L is the length of the side of the domain upon which the sinusoidal temperature is imposed, and B is the length of the other side of the rectangular domain. With a 50x50 discretization grid, the relative error of the numerical solution is smaller than $5x10^{-4}$ for the temperature, and $1x10^{-3}$ for the temperature derivatives.

The reference unsteady solution is the temperature field evolution in a rectangular domain, initially at temperature T_0, adiabatic on three sides and with a step temperature-change to zero on the fourth side. The evolution field is one-dimensional

Mesh size	Δτ	q[W/m^2]	%	Exec. time
56x60	6'	2.9329	-6.61%	33'18"
56x60	3'	2.8457	-3.45%	36'36"
56x60	45"	2.7709	-0.72%	47'56"
56x60	22"	2.7576	-0.24%	1h01'14"
56x60	10"	2.7508	0.00%	1h23'08"
56x60	5"	2.7489	0.07%	2h32'05"

Table 2 Time-step sensitivity analysis for CNC4 filled with polystyrene

	k [W/mK]	cρ [kJ/m^{3}K]	α [m^2/s]	β [Ws$^{0.5}$/m^{2}K]
CNC 1	0.120	400	0.30 x10^{-6}	219
CNC 2	0.250	800	0.31 x10^{-6}	447
CNC 3	0.410	1200	0.34 x10^{-6}	701
CNC 4	0.630	1600	0.39 x10^{-6}	1 004
Polystyrene	0.029	48	0.60 x10^{-6}	37
Mineral-wool	0.049	212	0.23 x10^{-6}	102

Table 3 Material characteristics

as none of the boundary conditions depends on the abscissa parallel to the non-adiabatic boundary, as given by [10]:

$$T(x,\tau) = \frac{2}{L}T_0\sum_{n=0}^{\infty} e^{-\lambda_n^2\alpha\tau}\sin(\lambda_n L)\cos(\lambda_n x) \tag{6}$$

where L is the length of the domain in the direction normal to the non-adiabatic face, and λ_n is the solution of equation:

$$\cos(\lambda_n L) = 0 \tag{7}$$

The series in eq. (6) is calculated numerically by neglecting the subseries whose terms have an absolute value lower than 10^{-6}. With a 50x50 discretization grid and a 1.25s time-step, the largest relative error of the numerical solution is less than 10^{-3}.

Tests on the dependence of the results on both grid-size and time-step have been performed for several combinations of the brick materials. The optimal grid-size and time-step used for computations are such that further refinements do not yield for noticeable modifications in the heat transfer rates, that is, the percentage changes of the peak heat flux is smaller than a prescribed accuracy value, i.e., 0.1%. The grid-size used for computations consists of 56x60 nodes, whilst the time-step is set to 10s. Selected results of the grid sensitivity analysis are presented in Table 1 for a CNC4 brick filled with polystyrene. Selected results of the time-step sensitivity analysis for the same brick are presented in Table 2 (notice that the refinement from 10" to 5" implies a percent change of the peak heat flux of only 0.07%, but the execution time increases drastically).

RESULTS AND DISCUSSION

Numerical simulations are performed for four types of concrete (denoted as CNC1 to CNC4), two insulation fillers, as well as the full block. The physical properties of the materials are reported in Table 3. In particular, the thermal conductivity, k, and the heat capacity per unit volume, cρ, are extracted from ref. [7], whilst the thermal diffusivity, α, and the thermal effusivity, β, are derived by their respective definition. Notice that the thermal diffusivity is only slightly increasing with density, whilst all the other properties increases remarkably passing from CMC1 to CNC4. In addition, it is worth pointing out that both insulation types have lower thermal conductivity and heat capacity per unit volume than CNC. Thus, all of them have necessarily lower thermal effusivity than any CNC. On the contrary, the thermal diffusivity of mineral-wool is slightly lower than that of any CNC, while the thermal diffusivity of polystyrene is almost the double than that of any CNC.

Thermal transmittance	CNC 1	CNC 2	CNC 3	CNC 4
Full brick	0.69	1.43	2.34	3.60
Mineral-wool	0.40	0.57	0.77	1.05
Polystyrene	0.30	0.47	0.67	0.94

Table 4 Thermal transmittance of the bricks [W/m^{2}K]

First of all, steady state simulations are carried out in order to determine the thermal transmittance of each of the twelve configurations examined, whose values are reported in Table 4. As expected, the lower is the thermal conductivity of both the masonry and the insulation material, the lower is the thermal transmittance of their combination.

The time-evolution of the temperature fields for, e.g., CNC1 bricks are delineated in Fig. 3. The contour plots highlight the differences between the role played by the mineral-wool and the polystyrene insulation. In fact, at the end of the pulse the highest temperature of both insulated bricks is higher than that of the full block. For the brick containing mineral-wool, this is due to a lower heat diffusion through the insulating filler. In contrast, for the brick with polystyrene, this is due to a higher heat diffusion in conjunction with a much lower heat capacity per unit volume. The lower thermal diffusivity of the mineral-wool with respect to polystyrene explains why the brick containing mineral-wool cools down more slowly than the brick containing polystyrene.

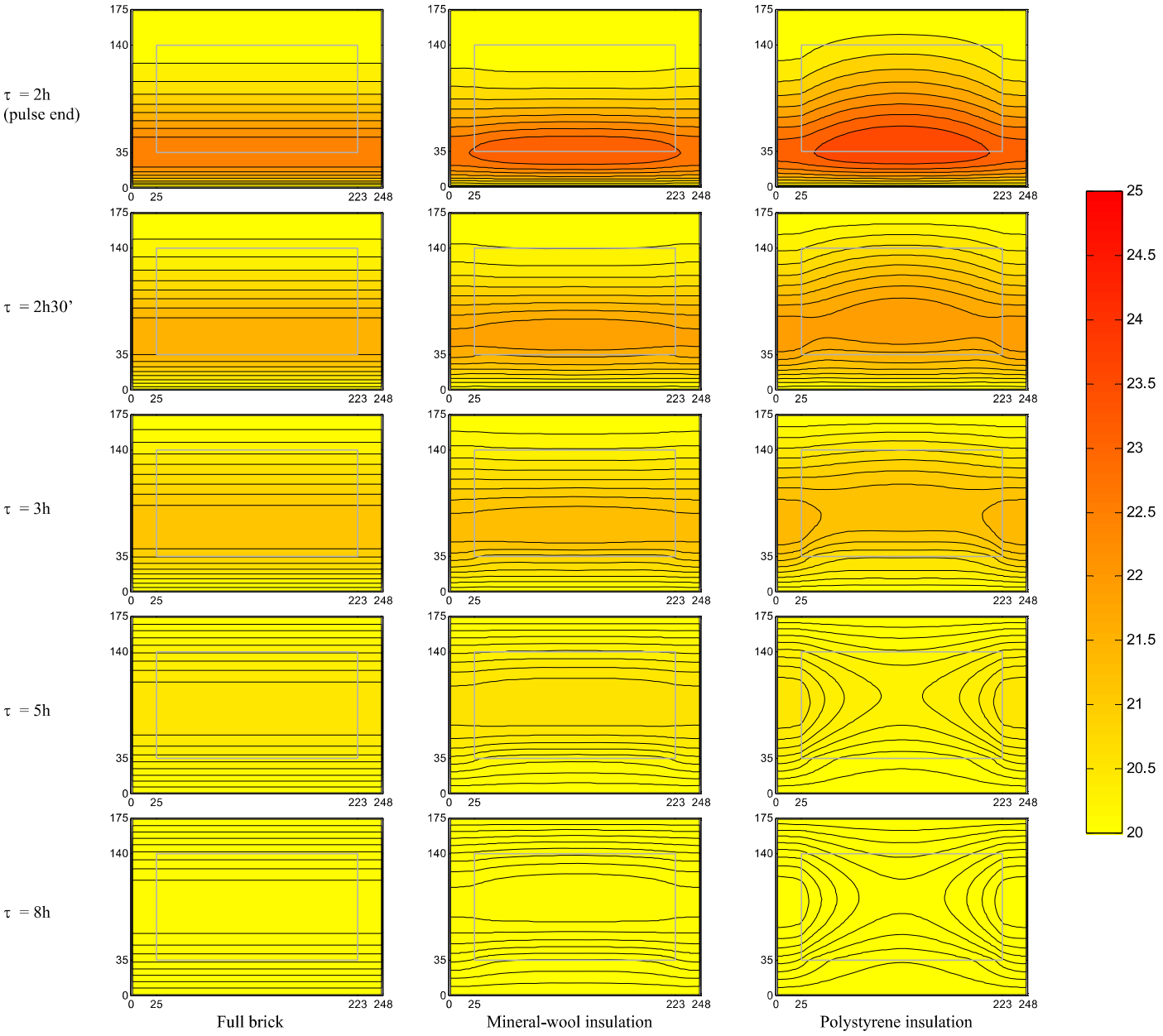

Figure 3 Temperature [°C] contour plots of CNC1 bricks full or insulated

The time-evolutions of the heat flux flowing through the face at constant temperature T_0 are reported in Fig. 4. It is apparent that the time-lag of the polystyrene-insulated brick is smaller than the other time-lags, whose values are almost the same. Moreover, the brick insulated by mineral-wool shows a slower drop off. Finally, the peak of the heat transfer rate distribution vs. time of the polystyrene-insulated brick is slightly higher than that of the brick containing mineral-wool, although the thermal transmittance of the former brick is lower than that of the latter.

The effect of the concrete type on the heat flux is reported in Figs. 5-7. The corresponding time-lags are shown in Fig. 8, where it is clear that, independently of the type of concrete, the polystyrene-insulated bricks have a time-lag lower than that of the full bricks. On the contrary, the bricks containing mineral-wool are characterized by time-lags that are slightly higher than those of the full bricks. Even more surprising is the fact that higher values of the front mass of the wall lead to lower time-lags, as displayed in Fig. 9. In Fig. 10, the distributions of the time-lag are also plotted versus the average thermal diffusivity of the brick, that is computed as the average of the thermal diffusivities of the frame and the core of the brick, weighted with the respective volume fractions. The analysis of this figure leads to conclude that the thermal diffusivity is the most important property which the time-lag depends on.

Finally, the values of the reciprocal of the decrement factor, defined as the ratio between the stationary heat flux and the transient maximum heat flux, are plotted against time-lag in Fig. 11. A multiple regression analysis of these data produces the following first-approach empirical correlating equation:

$$1/f = 0.35 + 1.627\Delta\tau_p \tag{8}$$

with a 3.2% standard deviation and a ±4.9% range of error.

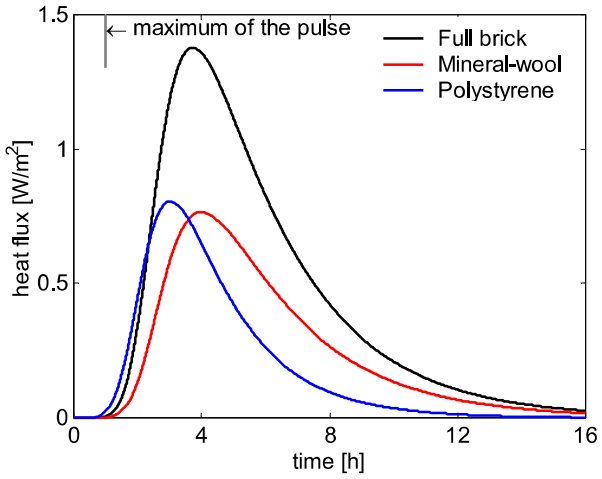

Figure 4 Heat flux vs. time for CNC1 bricks

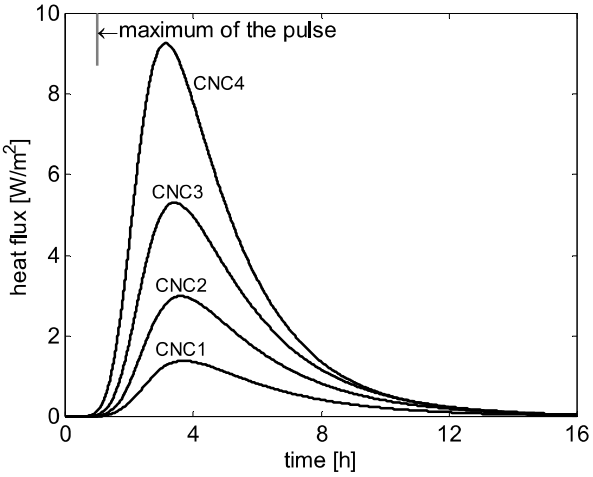

Figure 5 Heat flux vs. time for full bricks

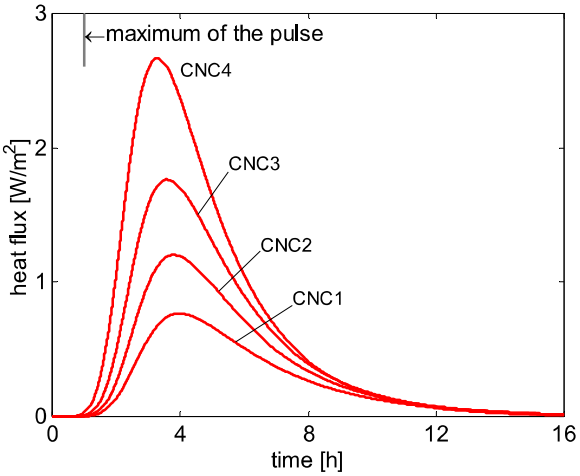

Figure 6 Heat flux vs. time for bricks filled with mineral-wool

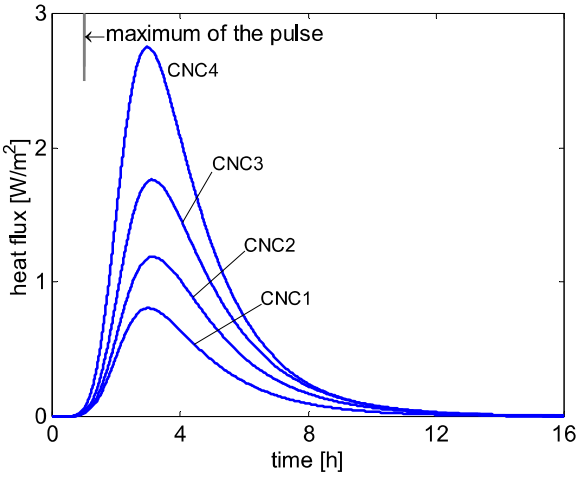

Figure 7 Heat flux vs. time for polystyrene insulated bricks

CONCLUSIONS

The response of insulated bricks to a triangular temperature-pulse has been studied numerically for different masonry and insulating materials.

The main results obtained may be summarized as follows:

- the heat flux response depends mainly on the average thermal diffusivity of the brick;
- the lower is the average thermal diffusivity, the higher is the time-lag;
- the time-lag is not a monotonous function of the wall front-mass;
- the decrement factor depends almost solely on the time-lag;
- the bricks insulated by mineral-wool have a steady-state and a transient performance higher than that of the full bricks.

However, it seems worth pointing out that the present paper is just a first-approach study and that much more work should be done in order to fully understand the unsteady behaviour of non-homogeneous building materials.

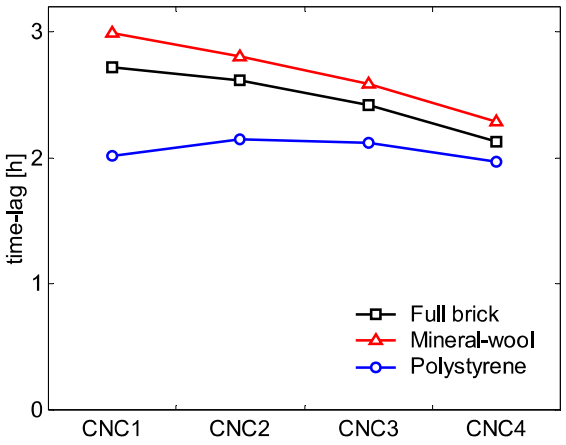

Figure 8 Time-lag for studied bricks vs. concrete type

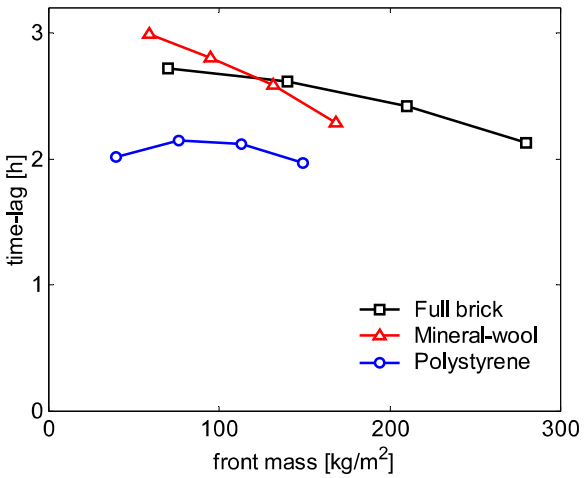

Figure 9 Time-lag vs. front mass

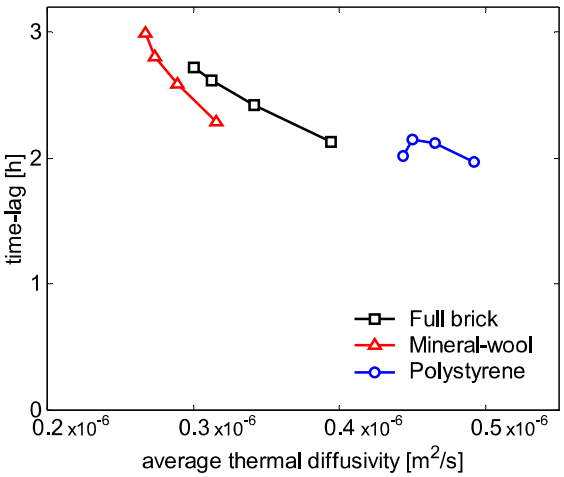

Figure 10 Time-lag vs. average thermal diffusivity

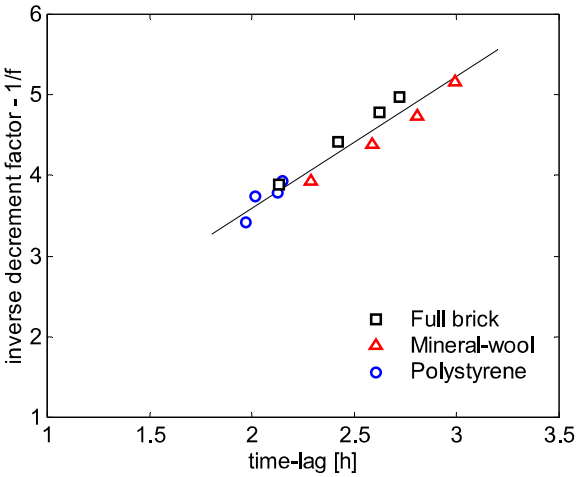

Figure 11 Decrement factor vs. time-lag for different insulating materials

NOMENCLATURE

c	[J / kg K]	Specific heat at constant pressure
f	[-]	*Decrement factor* – ratio between highest pulse heat transfer rate and steady state heat transfer rate
k	[W / m K]	Thermal conductivity
q	[W / m^2]	Heat flux
T	[K]	Temperature
x, y	[m]	Cartesian coordinates

Greek symbols

α	[m^2 / s]	Thermal diffusivity = k / c ρ
β	[W $s^{0.5}$/ m^2 K]	Thermal effusivity = $\sqrt{}$ k c ρ
ρ	[kg / m^3]	Density
τ	[s]	Time
$\Delta\tau$	[s]	Time-step
$\Delta\tau_p$	[h]	*Time-lag* – Time interval between the maximum of the temperature pulse and the highest heat flux through the brick face kept at constant temperature

REFERENCES

[1] ASHRAE Handbook of Fundamentals, Ch. 26, Atlanta, GA, USA (1993)

[2] B. Lacarrière, A. Trombe, F. Monochoux, Experimental unsteady characterization of heat transfer in a multi-layer wall including air layers – Application to vertically perforated bricks, *Energy and Buildings* 38 (2006) 232-237

[3] J.M. Sala, A. Urresti, K. Mrtìn, I. Flores, A. Apaolaza, Static and dynamic thermal characterisation of a hollow brick wall: Tests and numerical analysis, *Energy and Buildings* 40 (2008) 1513-1520

[4] K.C.K. Vijaykumar, P.S.S. Srinivasan, S. Dhandapani, A performance of hollow clay tile (HCT) laid reinforced cement concrete (RCC) roof for tropical summer climate, *Energy and Buildings* 39 (2007) 886-892

[5] Z.L. Zhang, B.J. Wachenfeldt, Numerical study on the heat storing capacity of concrete walls with air cavities, Energy and Buildings 41 (2009) 769-773

[6] G.H. Dos Santos, N. Mendes, Heat, air and moisture transfer through hollow porous blocks, Int. J. Heat Mass Transfer 52 (2009) 2390-2398

[7] EN 1745:2002 Masonry and masonry products – Methods for determining design thermal values

[8] D.G.Stephenson and G.P.Mitalas, Cooling Load Calculations by Thermal Response Factor Method, ASHRAE Transactions 73 (1967)

[9] L. Gori, Calcolo numerico (in Italian), Edizioni Kappa, Roma, Italy (1999)

[10] F. Kreith, Principles of Heat Transfer, DUN, New York, NY, USA (1973)